Original Paper

Cellular Physiology and Biochemistry

Cell Physiol Biochem 2005;16:15-22

Accepted: April 04, 2005

Thymocyte K^+, Na^+ and Water Balance During Dexamethasone- and Etoposide-Induced Apoptosis

Valentina E. Yurinskaya, Alexey V. Moshkov, Yuri M. Rozanov, Anna V. Shirokova, Irina O. Vassilieva, *Ekaterina V. Shumilina, *Florian Lang, Elena V. Volgareva, Alexey A. Vereninov

Institute of Cytology, Russian Academy of Sciences, St. Petersburg, *Department of Physiology, University of Tübingen

Key Words

Cell potassium • Sodium concentration • Water content • Apoptosis • Thymocytes

Abstract

The mechanism of apoptotic cell volume decrease was studied in rat thymocytes treated with dexamethasone (Dex) or etoposide (Eto). Cell shrinkage, i.e. dehydration, was quantified by using buoyant density of the thymocytes in a continuous Percoll gradient. The K^+ and Na^+ content of cells from different density fractions were assayed by flame emission analysis. Apoptosis was tested by microscopy and flow cytometry of acridine orange stained cells as well as by flow DNA cytometry. Treatment of the thymocytes with 1 μM Dex for 4-5.5 h or 50 μM Eto for 5 h resulted in the appearance of a new distinct high-density cell subpopulation. The cells from this heavy subpopulation but not those with normal buoyant density had typical features of apoptosis. Apoptotic increase of cell density was accompanied by a decrease in cellular K^+ content, which exceeded the simultaneous increase in cellular Na^+ content. Cellular loss of K^+ contributed to most of the estimated loss of cellular osmolytes, but owing to the parallel loss of cell water, the decrease in cytosolic K^+ concentration was less than one third. Due to gain of Na^+ and loss of cell water the cytosolic Na^+ concentration in thymocytes rose following treatment with Dex (5.5 h) or Eto (5 h) by a factor of about 3.6 and 3.1, respectively.

Introduction

Programmed cell death or apoptosis is a physiological mechanism providing removal of abundant, aged, defective, infected or potentially harmful cells [1-7]. Hallmarks of apoptosis include cell shrinkage which is considered to participate in the machinery eventually leading to cell death [8]. Accordingly, excessive osmotic cell shrinkage is a well known trigger of apoptosis [8, 9]. On the other hand, moderate osmotic cell shrinkage has been shown to impede CD95 induced apoptosis [10], pointing to a complex interaction of cell volume with apoptosis signaling.

Apoptotic cell volume decrease requires cellular loss of osmolarity [8]. In a variety of cells, apoptosis is indeed paralleled by activation of K^+ and/or Cl^- channels and loss of K^+, the major osmotically active intracellular

KARGER

Fax +41 61 306 12 34
E-Mail karger@karger.ch
www.karger.com

1015-8987/05/0163-0015$22.00/0

Accessible online at:
www.karger.com/journals/net

A.A. Vereninov
Institute of Cytology, Russian Academy of Sciences
St. Petersburg (Russia)
E-Mail veren@mail.cytspb.rssi.ru

component [4, 8, 11-20].

Apoptosis of Jurkat T lymphocytes following CD95 triggering or ceramide treatment is paralleled by activation of the outwardly rectifying Cl^- channel ORCC [21, 22], inhibition of Na^+/H^+ exchange [23], and release of the osmolyte taurine [15, 24], effects favouring apoptotic cell shrinkage [8]. Early cell shrinkage is, however, prevented by initial inhibition of Kv1.3 [21, 25], the cell volume regulatory K^+ channels of Jurkat lymphocytes [26]. Subsequent activation of Kv1.3 has been observed at a later stage of apoptosis [27] leading to eventual apoptotic cell shrinkage.

The influence of those events on intracellular electrolyte concentrations remained uncertain, as most preparations of apoptotic cells are heterogeneous and do not allow precise quantification of cellular electrolyte concentrations in a subset of cells. To overcome this limitation, we quantified alterations of cell water content by measuring buoyant density of cells in a continuous Percoll gradient and determined K^+ and Na^+ concentrations by flame emission analysis of cells extracted from Percoll layer of known density. Parallel determinations of cell water and ions allowed to estimate cytosolic K^+ and Na^+ concentrations and to assess the contribution of K^+ and Na^+ to apoptotic cell shrinkage.

We studied well-known models of apoptosis in rat thymocytes, such as the apoptosis induced by the glucocorticoid dexamethasone (Dex) [28-30] and the cytotoxic drug etoposide (Eto) [31-34]. Apoptosis was examined using microscopy and flow cytometry.

Materials and Methods

Cell culture

Thymus was isolated from decapitated 1-2 month old rats. Thymocytes were grown in RPMI 1640 medium (Biolot) supplemented with fetal bovine serum (10%, Biolot, St. Petersburg, Russia) and gentamicin G (100 µg/ml) and washed by two-fold centrifugation at 100 *g* in the same medium. Thymocytes at concentrations of 4-7 × 10^6 cells/ml were cultured at 37°C, 5% CO_2 for 4-6 h. Apoptosis was induced by dexamethasone phosphate (Dex; KRKA, Croatia) or etoposide (Eto; Sigma, Taufkirchen, Germany). Stock solutions of Dex (0.8 mM) and Eto (34 mM) in DMSO were added to yield final concentrations of the drugs of 1 µM and 50 µM, respectively. The final concentration of DMSO was 0.13 and 0.16%, respectively.

Analysis of cell water content

Cell water content was determined by measurements of buoyant density of cells in a continuous Percoll gradient (Pharmacia, New Jersey, USA). The Percoll solution was prepared by dilution of the initial stock solution with RPMI medium up to 40-55% and addition of the 10-fold volume of Hanks´ medium to maintain osmolarity. The density gradient was formed by centrifugation of the Percoll solution (2 ml) in 95-mm long tubes for 40 min at 2000 *g* (K-23 centrifuge, Janetzki, Germany). The density marker beads of 1.049, 1.062, 1.075, 1.087, and 1.098 g/ml (Sigma, Taufkirchen, Germany) were used for control of the gradient that was about 0.005 g/ml/cm. 100 µl of concentrated cell suspensions (20-50 × 10^6 thymocytes) were placed on the surface of the Percoll solution and centrifuged for 10 min at 400 *g* (MPW-340 centrifuge, CHEMARGO, Blachownia/Częstochowy, Poland). After isopyknic distribution of the cells in a density gradient, the fractions were collected by pipette and placed into 1.5 ml Eppendorf tubes. Then they were diluted 4-6 times with RPMI medium and spun for 5 min at 300 *g* (MPW-310 centrifuge, CHEMARGO, Blachownia/Częstochowy, Poland). Cells were resuspended in the RPMI medium and used for microscopy, flow cytometry, and determination of ion concentrations.

Water content per g protein, v_{prot}, was calculated as $v_{prot} = (1-\rho/\rho_{dry})/[0.65(\rho-1)]$, where ρ is the cell buoyant density and ρ_{dry} is the cell dry mass density taken as 1.45 g/ml. The ratio of protein to dry mass was taken as 0.65. The calculated water content could be higher or lower by about 10% if ρ_{dry} was taken as 1.50 or 1.40, respectively. Relative changes of cell water do not depend on the value of ρ_{dry} [35]. Buoyant density of cells is the most sensitive and reliable method for determination of cell water, as a difference in density by 0.005 g/ml that corresponds to a change in cell water content by about 10% leads to displacement of cells by approximately 1 cm in the gradient tube.

Determination of ion content

The cells were pelleted and washed in $MgCl_2$ solution (96 mM) 5 times without resuspension. The pellets were treated with 1 ml of 5% trichloroacetic acid (TCA) for 30 min and TCA-extracts were analyzed for $[K^+]$ and $[Na^+]$ by emission photometry in an air-propane flame using a Perkin-Elmer AA 306 spectrophotometer. Solutions of KCl and NaCl (10-100 µM) in 5% TCA were used as standard. TCA precipitates were dissolved in 0.1 N NaOH and assayed for protein by the Lowry procedure with serum bovine albumin as standard. The cell ion content was calculated in mmol per g of protein.

Flow cytometry

For staining with acridine orange (AO) and ethidium bromide (EB), 10^6/ml cells were incubated for 15-20 min at room temperature with AO (5 µg/ml) and EB (20 µg/ml). The forward light scattering (FLS) and fluorescence intensity at 530 ± 5 nm (F_{530}) and at > 620 nm (F_{620}) were determined using a flow cytometer equipped with a mercury arc lamp and a filter of 450-490 nm for fluorescence excitation and a Helium-Neon laser for determination of FLS [36]. For determination of cell DNA content the samples were placed into a solution containing 0.02% EDTA, 15 mM $MgCl_2$, 0.1% Triton X-100, 20 µg/ml EB and 40 µg/ml oligomycin, pH 7.4, for 20-24 h at 4-6°C. Fluorescence was measured at > 600 nm with excitation at 380-470 nm, using flow cytometry [37].

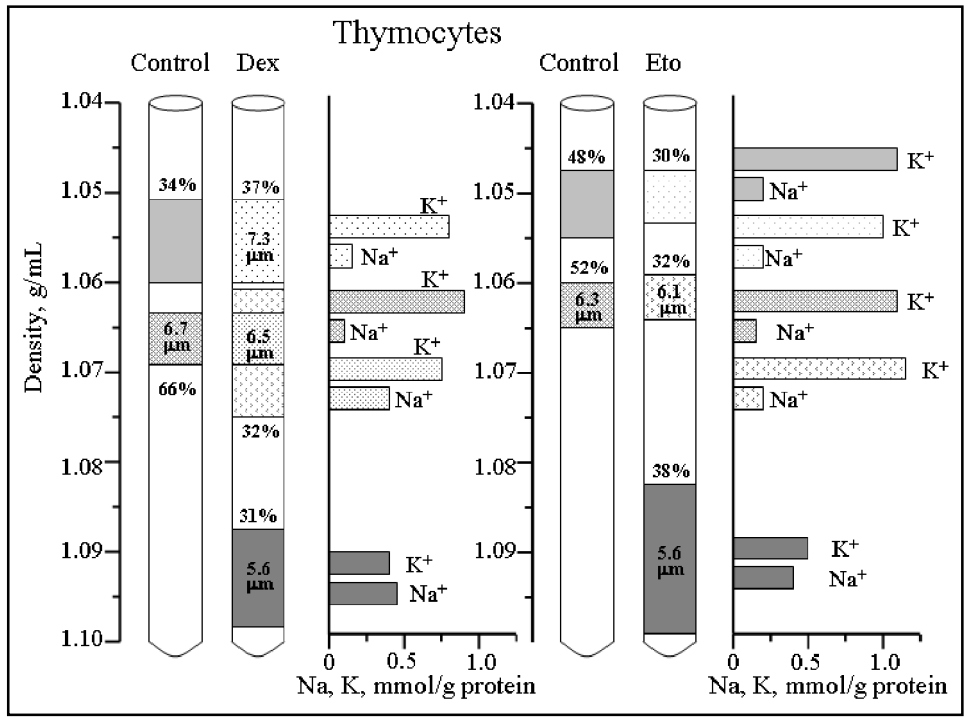

Fig. 1. Distribution of normal and apoptotic thymocytes in continuous Percoll density gradient and ion content of thymocytes from different fractions. Thymocytes were treated with 1 µM Dex for 5.5 h or with 50 µM Eto for 5 h. *Horizontal axis* – ion content, mmol/g protein. *Vertical axis* – density, g/ml. The position of cell subpopulations in tubes with density gradient (L = light, M = middle, H = heavy) and their ion contents are shown. Ion content in cells of the middle subpopulation of thymocytes treated with Dex was obtained for cells with the same buoyant density as the control subpopulation with similar density (M). Figures next to the bars represent the relative size of the respective subpopulation in % of cellular protein. The mean thymocyte diameter (µm) is given inside the bars. Two separate experiments.

Microscopy

Cell preparations were stained with AO and EB (similar to that used for flow cytometry). Fluorescence and light microscopy of the vital cell preparations were obtained using a Mikmed-2 microscope (LUMAM PRO-11, LOMO, Russia) supplemented with a CCD-camera and the filter set "Green". The cell size was determined by the area of maximal cell projection (S), which was determined utilizing the IMAGEJ program (NIH, USA). The diameter was calculated from the formula $d = 2(S/\pi)^{1/2}$. Cells that were positively stained with EB were excluded.

Statistical analysis

Results were analyzed by Student's *t* test and considered statistically significantly different at $p < 0.05$.

Results

Cell water content

Fig. 1 illustrates the distribution of thymocytes in density gradient tubes before and after incubation of cells with either Dex (1 µM, 5.5 h) or Eto (50 µM, 5 h). A separate subpopulation of thymocytes with an increased density appeared approaching protein portion of 31% upon treatment with Dex, while 38%, after treatment with Eto. The mean percentage of cell protein content in the Dex and Eto apoptotic fraction were 31 ± 2% ($n = 9$) and 38 ± 8% ($n = 5$), respectively. The mean values of buoyant density for different thymocyte subpopulations are presented in Table 1. The water content per g of cell protein in the M fractions of the control thymocytes was found to be 5.6-6.1 ml/g depending on the rat. It dropped to 4.1 and 4.2 ml/g in the apoptotic H thymocytes treated with Dex and Eto, respectively. Comparison of apoptosis after the 4- and 5.5-h incubation of thymocytes of the same rats showed no statistically significant differences in buoyant density or the cell K^+ and Na^+ content.

Apoptosis was examined by flow cytometry and microscopy. Apoptosis of thymocytes treated with Dex or Eto was evident from an increase of the subG1 component, by a sharp increase of fragmentation (Fr) in the DNA histogram (Fig. 2), by changes in the two-dimensional Red/Green flow cytogram obtained for viable thymocytes stained with AO, and by a decrease of cell diameters measured under microscope (Fig. 1). Cells from the heavy subpopulation H differed by all these characteristics from the cells with buoyant density corresponding to that in control cells (L and M fractions). The number of nonviable cells that could be stained by ethidium bromide in the H fraction did not differ from that in the L and M fractions. Invariably more cells in the S-phase were found in the L fractions than in the M fractions (Table 1).

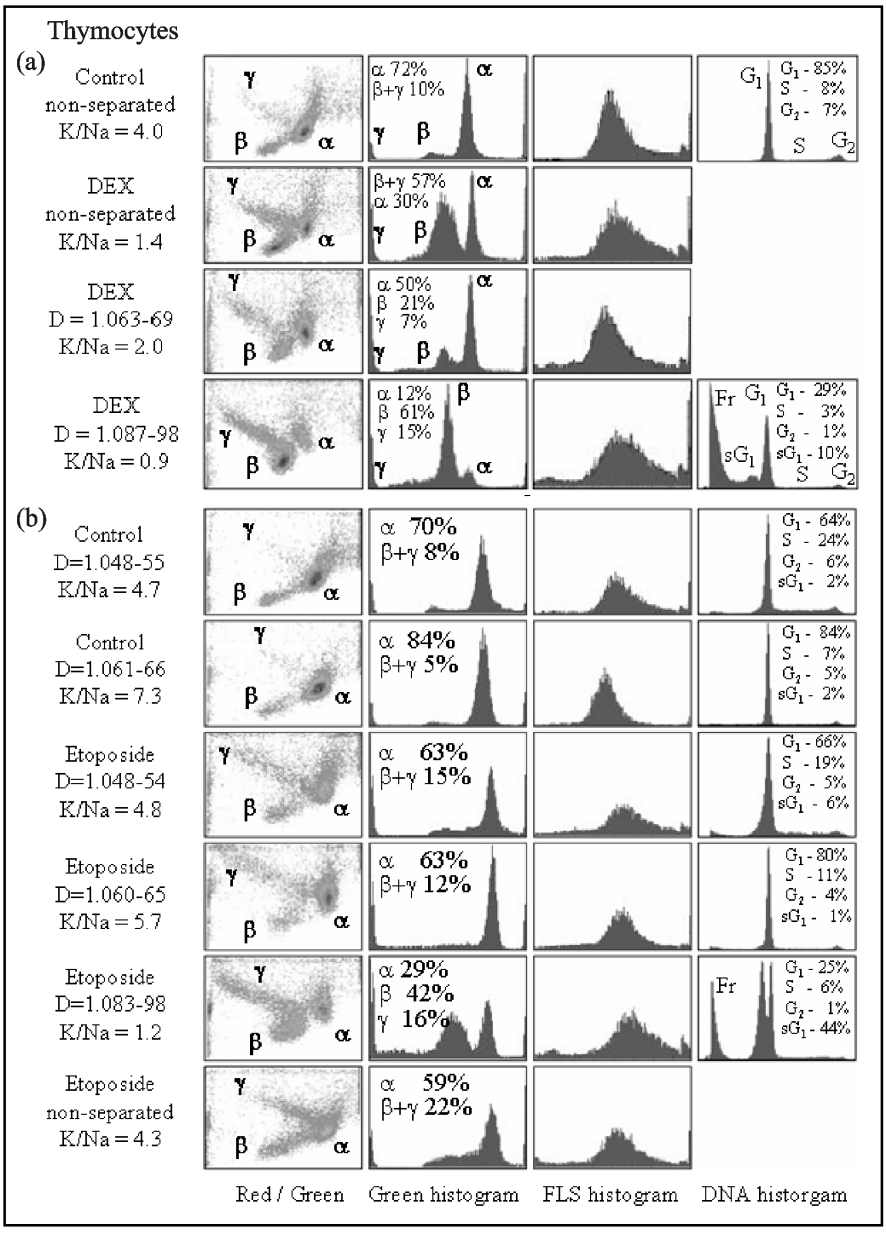

Fig. 2. Flow cytometry of thymocytes treated with Dex (a*)* or with Eto (b*)*. The data were obtained in the same experiments as in Fig. 1. *Horizontal axis* – fluorescence at 530 nm in two-dimensional Red/Green histograms (outer left), one-dimensional Green histograms (middle left), forward light scattering in FLS histograms (middle right), and amount of DNA according to EB fluorescence in DNA histograms (outer right). *Vertical axis* – fluorescence at 620 nm in two-dimensional Red/Green histograms or the cell number in one-dimensional histograms. Symbols α, β, γ, G_1, sG_1, S, and G_2 designate cell subpopulations selected on the Red/Green, Green fluorescence, and DNA histograms. The Red/Green and Green histograms were obtained on cells stained with AO and EB. Buoyant densities (D) and K^+/Na^+ ratios (K/Na) for the respective cell populations are given on the left of the graphs.

Cellular ion content

Apoptotic increase in cell density pointing to cell dehydration was accompanied by a decrease of cytosolic K^+ and an increase of cytosolic Na^+ (Table 1). The K^+/Na^+ ratio decreased from 4.6-6.3 in the control thymocytes of fraction M to 1.0-1.3 in apoptotic cells of fraction H. Most importantly, the K^+ loss exceeded the accompanying Na^+ accumulation. Therefore, the sum of K^+ and Na^+ contents decreased by about 0.24 mmol/g protein in thymocytes treated for 5.5 h with Dex and by 0.32 mmol/g protein in thymocytes treated with Eto. Apoptotic loss of cell water (volume) under permanent osmotic equilibrium between cell and medium implies isoosmotic exit of intracellular solutes and water. In view of the amount of water lost and the osmolality of the medium taken as 315 mosmol/l the total osmolyte loss should be 0.57 mmol/g in the apoptotic thymocytes treated with Dex for 5.5 h and 0.60 mmol/g in thymocytes treated with Eto. Therefore, 42-53% of the apoptotic decrease in the amount of intracellular osmolytes should be due to the redistribution of K^+ and Na^+. The overall contribution of ions to apoptotic cell shrinkage could approach 84-100%, if the displacement of K^+ and Na^+ were accompanied by an equivalent loss of monovalent anions such as Cl^- and $H_2PO_4^-$.

The buoyant density, i.e. water content, in thymocytes of the L and M fractions also correlated with the total cellular K^+ and Na^+ content ($R = 0.786$, $SD = 0.533$, $P = 8.7 \times 10^{-4}$). Following Dex treatment the thymocytes from the L and M fractions showed a small but statistically significant decrease in the K^+ content and in the K^+/Na^+ ratio as compared with the same fractions of the control population. This effect may be considered as the "preapoptotic" alteration of thymocytes before the stepwise transition into the dense fraction H.

Cells, fractions	Buoyant density of cells, ρ, g / mL	Water, mL/g protein	K^+, mmol/g protein	Na^+, mmol/g protein	$[K^+]$, mM	$[Na^+]$, mM	K^+/Na^+	DNA cytometry data		
								S/G_1	G_2/G_1	Fr, %
Control L	1.051 - 1.063 (11)	7.3	0.98±0.04	0.25±0.02	134	34	3.6±0.5 (11)	0.24±0.01 (4)	0.08±0.01	1.9±0.5
Control M	1.064 - 1.073 (11)	5.9	0.90±0.02	0.17±0.01 [b]	152	29	5.6±0.4 (12) [b]	0.07±0.02 (5) [b]	0.07±0.01	1.6±0.3
Dex L	1.053 - 1.064 (9)	7.1	0.82±0.01 [a]	0.26±0.01	115	37	3.2±0.2 (9)	0.25±0.01 (3)	0.07±0.01	2.9±0.6
Dex M	1.065 - 1.074 (9)	5.8	0.74±0.01 [a]	0.25±0.02 [a]	127	43	3.3±0.3 (9) [a]	0.06±0.01 (4) [b]	0.06±0.01	3.0±0.2
Dex H 5.5h	1.086 - 1.100 (9)	4.1	0.41±0.03 [a]	0.42±0.02 [a]	101	103	1.0±0.1 (9) [a]	0.11±0.02 (4)	0.03±0.004 [a]	41±6.0 [a]
Control L	1.056 - 1.066 (3)	6.8	0.92±0.11	0.24±0.03	135	36	4.1±0.9 (3)			
Control M	1.068 - 1.076 (3)	5.6	0.86±0.03	0.21±0.05	152	38	4.6±1.1 (3)			
Dex L	1.056 - 1.066 (3)	6.8	0.77±0.06	0.33±0.01	114	49	2.4±0.3 (3)			
Dex M	1.067 - 1.076 (3)	5.6	0.75±0.11	0.29±0.08	134	52	3.2±1.0 (3)			
Dex H 4h	1.086 - 1.100 (3)	4.1	0.55±0.08 [a]	0.51±0.05 [a]	135	125	1.2±0.2 (3) [a]			
Dex L	1.055 - 1.066 (3)	6.8	0.83±0.02	0.27±0.01	122	40	3.1±0.1 (3)			
Dex M	1.068 - 1.075 (3)	5.6	0.76±0.02	0.22±0.01	135	39	3.4±0.3 (3)			
Dex H 5.5h	1.086 - 1.100 (3)	4.1	0.49±0.08 [a]	0.39±0.01 [a]	120	96	1.3±0.3 (3) [a]			
Control L	1.049 - 1.059 (5)	7.8	0.95±0.09	0.24±0.05	122	31	4.5±0.7 (5)	0.36±0.04 (5)	0.09±0.01	3.6±0.8
Control M	1.063 - 1.070 (5)	6.1	0.94±0.04	0.17±0.03 [b]	154	28	6.3±0.9 (5)	0.07±0.01 (5) [b]	0.05±0.01	2.9±0.4
Eto L	1.049 - 1.057 (5)	8.0	0.93±0.05	0.29±0.04	117	36	3.5±0.5 (5)	0.32±0.02 (5)	0.10±0.02	6.6±1.3
Eto M	1.061 - 1.067 (5)	6.0	0.91±0.07	0.25±0.03	153	42	3.9±0.5 (5) [a]	0.11±0.01 (3) [b]	0.07±0.01	6.2±1.0
Eto H	1.082 - 1.098 (5)	4.2	0.42±0.02 [a]	0.37±0.03 [a]	99	87	1.2±0.1 (5) [a]	0.20±0.04 (3) [a]	0.03±0.01	37±5.6 [a]

Table 1. Water, K^+, and Na^+ contents and ion concentrations in cell water in rat thymocytes under apoptosis induced by dexamethasone (Dex) or etoposide (Eto). Water content per g protein, $v_{prot.}$, was calculated as $v_{prot.} = (1-\rho/\rho_{dry})/[0.65(\rho-1)]$, taking the density of cell dry mass, ρ_{dry}, to be 1.45 g/mL and the proportion of protein in the dry mass to be 65 %. Means ± SEM. Number of experiments, n, is indicated in parentheses. The thymocytes were treated by 1 μM Dex for 4 or 5.5 h or 50 μM etoposide for 4.5-5 h. The data for comparison of 4 and 5.5 h incubation were obtained in the parallel experiments with thymocytes of the same rats.

[a] the difference from the appropriate control value is significant at $P < 0.05$; [b] the difference from the control fraction L value is significant at $P < 0.05$.

Cell ion concentrations

Intracellular K^+ and Na^+ concentrations calculated from cell water and cation content per g of protein are shown in Table 1. The K^+ concentration per cell water after treatment with Dex (5.5 hours) or Eto (4 hours) decreased by about 34 and 36%, respectively. The Na^+ concentrations under the same conditions increased by a factor of 3.6 and 3.1, respectively. The relative increase in the Na^+ concentration in apoptotic thymocytes was significantly more pronounced than the decrease in the K^+ concentration, as entry of Na^+ paralleled the exit of water. It is to be pointed out that the relative changes of the cell water content estimated from measurements of buoyant density and thus the estimated alterations of cellular K^+ concentration do not depend significantly on dry mass density.

Discussion

Isolation of apoptotic thymocytes by isopyknic centrifugation on density gradient has been used in the study of apoptosis for a long time [38-40]. Separation of thymocytes into distinct fractions according to their apoptosis susceptibility and a stepwise kinetics of the thymocyte transition to apoptosis were shown by flow cytometry and other methods [41-43]. Experiments with continuous Percoll gradients like in Fig. 1 also allowed to segregate sensitive from resistant thymocytes. Using a continuous density gradient, we were able to estimate simultaneously the intracellular water and ion contents of thymocytes from different subsets. By this way, a pronounced increase of Na^+ concentration and a relatively small decrease of cytosolic K^+ concentration were found in apoptotic thymocytes.

Previous estimates of cellular ion concentrations during apoptosis used predominantly indirect approaches and were qualitative rather than quantitative. Several studies were based on determination of changes in the cellular K^+ content with use of fluorescent probes PBFI and SBFI and of changes in the cell size by light scattering or by a Coulter counter [11, 43-47]. Earlier, Hughes and collaborators [46] measured cellular K^+ content in thymocytes during the Dex-induced apoptosis (1 μM, 2-8 h), using the K^+ sensitive fluorescent probe PBFI in flow cytometry, utilizing mass-spectrometry, and applying atomic absorption. They revealed a 95% reduction of the PBFI fluorescence intensity in the subpopulation of

apoptotic thymocytes selected by forward and side light scattering and a decrease of K^+ concentration in the apoptotic thymocyte subpopulation from 140 mM to 35 mM in control cells. In another study [11], the K^+ content in Jurkat cells during apoptosis induced by anti-Fas antibody was determined using the same methods. Only shrunken, i.e. apoptotic cells showed a decrease of fluorescence of the K^+-sensitive PBFI probe. No quantitative estimates of the K^+ content per cell or concentration per cell water were carried out in this as well as in the later studies from the same laboratory [48]. A decrease of PBFI fluorescence in mouse thymocytes following induction of apoptosis by Dex was further observed by Dallaporta and colleagues [45] demonstrating that the K^+ content per cell assessed by flame photometry dropped in apoptotic cells down to 1/3 of the value in normal thymocytes, a value approached even in a subpopulation of cells with normal forward and side light scattering. Using flame photometry for determination of K^+ and radioisotopes for evaluation of intra- and extracellular water, Benson et al. [49] studied apoptosis of lymphoblastoid CEM cells treated with Dex and reported a decrease of the K^+ content per cell by 15% and the same reduction in cell volume estimated using a Coulter counter in spite of no increase in cell buoyant density during the first 24 h of apoptosis. The K^+ concentration in cell water found to be 305 mM in normal and 270 mM in apoptotic cells seems too high in view of the total osmolality of external media amounting to 300-315 mosmol/l.

A marked decrease in the K^+ content and K^+/Na^+ ratio in apoptotic cells of different species were shown with the aid of an X-ray elemental microanalysis [50-55]. In parallel with the decrease of the total K^+ and Na^+ content, a pronounced reduction in the Cl and P content was also found in apoptotic human monocytes [54]. As apoptosis and necrosis are both associated with a decrease in the K^+/Na^+ ratio, the differences of element ratios may not allow the discrimination between those two types of cell death [52]. According to our observations, the sum of K^+ and Na^+ contents is lower in shrunken apoptotic cells *vs* normal cells. In contrast the sum should be higher in swollen necrotic cells. Indeed, a decrease in the sum of K^+ and Na^+ contents in apoptotic cells was observed when apoptosis was confirmed by other markers. However, the quantitative analysis of the relationship between cell shrinkage and a decrease in cell K^+ content found in the X-ray microanalysis studies is impeded by difficulties in determination of the amount of cell water.

We believe that our study of the relationship between changes of cell water and ion content during apoptosis is based on more reliable estimates than flow cytometry alone or X-ray microanalysis. The data obtained confirm a concept that the decrease in potassium content is one of the most significant factors leading to apoptotic cell shrinkage. Since the loss of K^+ is paralleled by a similar loss of cell water, the cytosolic K^+ concentration decreased only by about one third. Our estimates of the cellular K^+ concentration during apoptotic shrinkage appeared to contradict the suggestion that a decrease in intracellular K^+ concentration plays a key role in regulation of apoptotic enzymes, e.g. nucleases and caspases [56, 57]. The observed decrease of intracellular K^+ concentration found in the apoptotic thymocytes in our experiments is smaller than the decrease of K^+ concentrations required to significantly modify activity of these enzymes in cell-free systems. It should be kept in mind, however, that the K^+ sensitivity of the enzymes may be modified by other cellular components and that the sensitivity in cell free systems may not quantitatively reflect the intracellular effect of K^+ on the enzymes. Nevertheless, apoptotic changes in cytosolic Na^+ concentration are much more pronounced than those in K^+ concentration and may well contribute to the stimulation of apoptosis [13].

To the extent that the loss of cations is paralleled by the loss of monovalent anions such as Cl^- and $H_2PO_4^-$, the share of the monovalent ions in the total loss of cell osmolytes underlying the apoptotic loss of cell water would be dominant. However, apoptotic death is paralleled by cytosolic acidification [23, 58] that decreases the negative charge of proteins and thereby contributes to loss of cellular anions. Thus, the exit of K^+ is presumably not matched by similar exit of monovalent anions. The cellular loss of osmolarity may at least partially be due to release of organic osmolytes, similar to CD95 induced apoptosis of Jurkat T lymphocytes [8, 15] or glial cells [59]. Interestingly, lack of the taurine transporter TAUT interferes with apoptosis of erythrocytes [60].

Acknowledgements

This work was supported by the Russian Foundation for Basic Research (project 01-04-49111) and the Deutsche Forschungsgemeinschaft (436 RUS 113/488/0-2R). The authors acknowledge the meticulous preparation of the manuscript by Lejla Subasic and Tanja Loch.

References

1 Bergamo P, Luongo D, Rossi M: Conjugated linoleic acid-mediated apoptosis in Jurkat T cells involves the production of reactive oxygen species. Cell Physiol Biochem 2004;14:57-64.

2 Brand VB, Sandu CD, Duranton C, Tanneur V, Lang KS, Huber SM, Lang F: Dependence of Plasmodium falciparum in vitro growth on the cation permeability of the human host erythrocyte. Cell Physiol Biochem 2003;13:347-356.

3 Grassme H, Kirschnek S, Riethmueller J, Riehle A, von Kurthy G, Lang F, Weller M, Gulbins E: CD95/CD95 ligand interactions on epithelial cells in host defense to Pseudomonas aeruginosa. Science 2000;290:527-530.

4 Gulbins E, Jekle A, Ferlinz K, Grassmé H, Lang F: Physiology of apoptosis. Am J Physiol Renal Physiol 2000;279:F605-F615.

5 Long H, Han H, Yang B, Wang Z: Opposite cell density-dependence between spontaneous and oxidative stress-induced apoptosis in mouse fibroblast L-cells. Cell Physiol Biochem 2003;13:401-414.

6 Sturm J, Zhang H, Magdeburg R, Hasenberg T, Bönninghoff R, Oulmi J, Keese M, McCuskey R: Altered Apoptotic Response and Different Liver Structure During Liver Regeneration in FGF-2-Deficient Mice. Cell Physiol Biochem 2004;14:249-260.

7 Walsh MF, Thamilselvan V, Grotelueschen R, Farhana L, Basson M: Absence of adhesion triggers differential FAK and SAPKp38 signals in SW620 human colon cancer cells that may inhibit adhesiveness and lead to cell death. Cell Physiol Biochem 2003;13:135-146.

8 Lang F, Busch GL, Ritter M, Völkl H, Waldegger S, Gulbins E, Häussinger D: Functional significance of cell volume regulatory mechanisms. Physiol Rev 1998;78:247-306.

9 Rosette C, Karin M: Ultraviolet light and osmotic stress: activation of the JNK cascade through multiple growth factor and cytokine receptors. Science 1996;274:1194-1197.

10 Gulbins E, Welsch J, Lepple-Wienhuis A, Heinle H, Lang F: Inhibition of Fas-induced apoptotic cell death by osmotic cell shrinkage. Biochem Biophys Res Commun 1997;236:517-521.

11 Bortner CD, Cidlowski JA: Caspase independent/dependent regulation of K(+), cell shrinkage, and mitochondrial membrane potential during lymphocyte apoptosis. J Biol Chem 1999;274:21953-21962.

12 Bortner CD, Cidlowski JA: Apoptotic volume decrease and the incredible shrinking cell. Cell Death Differ 2002;9:1307-1310.

13 Bortner CD, Cidlowski JA: The role of apoptotic volume decrease and ionic homeostasis in the activation and repression of apoptosis. Pflugers Arch 2004;448:313-318.

14 Han H, Wang J, Zhang Y, Long H, Wang H, Xu D, Wang Z: HERG K channel conductance promotes H2O2-induced apoptosis in HEK293 cells: cellular mechanisms. Cell Physiol Biochem 2004;14:121-134.

15 Lang F, Ritter M, Gamper N, Huber S, Fillon S, Tanneur V, Lepple-Wienhues A, Szabo I, Gulbins E: Cell volume in the regulation of cell proliferation and apoptotic cell death. Cell Physiol Biochem 2000;10:417-428.

16 Maeno E, Ishizaki Y, Kanaseki T, Hazama A, Okada Y: Normotonic cell shrinkage because of disordered volume regulation is an early prerequisite to apoptosis. Proc Natl Acad Sci U S A 2000;97:9487-9492.

17 Myssina S, Lang P, Kempe D, Kaiser S, Huber S, Wieder T, Lang F: Cl Channel Blockers NPPB and Niflumic Acid Blunt Ca(2+)-induced Erythrocyte 'Apoptosis'. Cell Physiol Biochem 2004;14:241-248.

18 Okada Y, Maeno E, Shimizu T, Dezaki K, Wang J, Morishima S: Receptor-mediated control of regulatory volume decrease (RVD) and apoptotic volume decrease (AVD). J Physiol 2001;532:3-16.

19 Yu SP, Canzoniero LM, Choi DW: Ion homeostasis and apoptosis. Curr Opin Cell Biol 2001;13:405-411.

20 Yu SP: Regulation and critical role of potassium homeostasis in apoptosis. Prog Neurobiol 2003;70:363-386.

21 Gulbins E, Szabó I, Baltzer K, Lang F: Ceramide-induced inhibition of T lymphocyte voltage-gated potassium channel is mediated by tyrosine kinases. Proc Natl Acad Sci U S A 1997;94:7661-7666.

22 Szabó I, Lepple-Wienhues A, Kaba KN, Zoratti M, Gulbins E, Lang F: Tyrosine kinase-dependent activation of a chloride channel in CD95-induced apoptosis in T lymphocytes. Proc Natl Acad Sci U S A 1998;95:6169-6174.

23 Lang F, Madlung J, Bock J, Lükewille U, Kaltenbach S, Lang KS, Belka C, Wagner CA, Lang HJ, Gulbins E, Lepple-Wienhues A: Inhibition of Jurkat-T-lymphocyte Na+/H+-exchanger by CD95(Fas/Apo-1)-receptor stimulation. Pflugers Arch 2000;440:902-907.

24 Lang F, Madlung J, Uhlemann AC, Risler T, Gulbins E: Cellular taurine release triggered by stimulation of the Fas(CD95) receptor in Jurkat lymphocytes. Pflugers Arch 1998;436:377-383.

25 Szabó I, Gulbins E, Apfel H, Zhang X, Barth P, Busch AE, Schlottmann K, Pongs O, Lang F: Tyrosine phosphorylation-dependent suppression of a voltage-gated K+ channel in T lymphocytes upon Fas stimulation. J Biol Chem 1996;271:20465-20469.

26 Deutsch C, Chen LQ: Heterologous expression of specific K+ channels in T lymphocytes: functional consequences for volume regulation. Proc Natl Acad Sci U S A 1993;90:10036-10040.

27 Storey NM, Gómez-Angelats M, Bortner CD, Armstrong DL, Cidlowski JA: Stimulation of Kv1.3 potassium channels by death receptors during apoptosis in Jurkat T lymphocytes. J Biol Chem 2003;278:33319-33326.

28 Enomoto R, Sugahara C, Tsuda Y, Okada Y, Lee E: Thymocyte Apoptosis Induced by Various Compounds Including YO-2 Is Accompanied by a Change in Chromatin Structure. Ann N Y Acad Sci 2004;1030:622-626.

29 Lei HY, Tang MJ, Tsao N: Intracellular alkalinization in dexamethasone-induced thymocyte apoptosis. Apoptosis 1997;2:304-312.

30 Tonomura N, McLaughlin K, Grimm L, Goldsby RA, Osborne BA: Glucocorticoid-induced apoptosis of thymocytes: requirement of proteasome-dependent mitochondrial activity. J Immunol 2003;170:2469-2478.

31 Martinsson P, Liminga G, Nygren P, Larsson R: Characteristics of etoposide-induced apoptotic cell death in the U-937 human lymphoma cell line. Anticancer Drugs 2001;12:699-705.

32 Plo I, Hernandez H, Kohlhagen G, Lautier D, Pommier Y, Laurent G: Overexpression of the atypical protein kinase C zeta reduces topoisomerase II catalytic activity, cleavable complexes formation, and drug-induced cytotoxicity in monocytic U937 leukemia cells. J Biol Chem 2002;277:31407-31415.

33 Saeki K, Kobayashi N, Inazawa Y, Zhang H, Nishitoh H, Ichijo H, Saeki K, Isemura M, Yuo A: Oxidation-triggered c-Jun N-terminal kinase (JNK) and p38 mitogen-activated protein (MAP) kinase pathways for apoptosis in human leukaemic cells stimulated by epigallocatechin-3-gallate (EGCG): a distinct pathway from those of chemically induced and receptor-mediated apoptosis. Biochem J 2002;368:705-720.

34 Umeda T, Kouchi Z, Kawahara H, Tomioka S, Sasagawa N, Maeda T, Sorimachi H, Ishiura S, Suzuki K: Limited proteolysis of filamin is catalyzed by caspase-3 in U937 and Jurkat cells. J Biochem (Tokyo) 2001;130:535-542.

35 Vereninov AA, Volgareva EV, Matveev VV, Moshkov AV, Rozanov I, Shirokova AV, Iurinskaia VE: Water and ion balance in rat thymocytes under apoptosis induced with dexamethasone or etoposide. Ion-osmotic model of cell volume decrease. Tsitologiia 2003;45:500-509.
36 Lonskaya IA, Volgareva EV, Rozanov YM: Two different types of apoptosis in thymocytes. Tsitologiia 2001;43:244-249.
37 Rozanov I, Vinogradov AE: [Precise DNA cytometry: investigation of individual variability in animal genome size]. Tsitologiia 1998;40:792-800.
38 Thomas N, Bell PA: Glucocorticoid-induced cell-size changes and nuclear fragility in rat thymocytes. Mol Cell Endocrinol 1981;22:71-84.
39 Wyllie AH, Morris RG: Hormone-induced cell death. Purification ad properties of thymocytes undergoing apoptosis after glucocorticoid treatment. Am J Pathol 1982;109:78-87.
40 Yamada T, Ohyama H: Separation of the dead cell fraction from X-irradiated rat thymocyte suspensions by density gradient centrifugation. Int J Radiat Biol Relat Stud Phys Chem Med 1980;37:695-699.
41 Chow SC, Snowden R, Orrenius S, Cohen GM: Susceptibility of different subsets of immature thymocytes to apoptosis. FEBS Lett 1997;408:141-146.
42 Cohen GM, Sun XM, Snowden RT, Ormerod MG, Dinsdale D: Identification of a transitional preapoptotic population of thymocytes. J Immunol 1993;151:566-574.
43 Hughes FM, Jr., Cidlowski JA: Glucocorticoid-induced thymocyte apoptosis: protease-dependent activation of cell shrinkage and DNA degradation. J Steroid Biochem Mol Biol 1998;65:207-217.
44 Barbiero G, Duranti F, Bonelli G, Amenta JS, Baccino FM: Intracellular ionic variations in the apoptotic death of L cells by inhibitors of cell cycle progression. Exp Cell Res 1995;217:410-418.
45 Dallaporta B, Hirsch T, Susin SA, Zamzami N, Larochette N, Brenner C, Marzo I, Kroemer G: Potassium leakage during the apoptotic degradation phase. J Immunol 1998;160:5605-5615.
46 Hughes FM, Jr., Bortner CD, Purdy GD, Cidlowski JA: Intracellular K+ suppresses the activation of apoptosis in lymphocytes. J Biol Chem 1997;272:30567-30576.
47 McCarthy JV, Cotter TG: Cell shrinkage and apoptosis: a role for potassium and sodium ion efflux. Cell Dearth Differ 1997;4:756-770.
48 Gómez-Angelats M, Bortner CD, Cidlowski JA: Protein kinase C (PKC) inhibits fas receptor-induced apoptosis through modulation of the loss of K+ and cell shrinkage. A role for PKC upstream of caspases. J Biol Chem 2000;275:19609-19619.
49 Benson RS, Heer S, Dive C, Watson AJ: Characterization of cell volume loss in CEM-C7A cells during dexamethasone-induced apoptosis. Am J Physiol 1996;270:C1190-C1203.
50 Fernández-Segura E, Canizares FJ, Cubero MA, Warley A, Campos A: Changes in elemental content during apoptotic cell death studied by electron probe X-ray microanalysis. Exp Cell Res 1999;253:454-462.
51 Offen D, Ziv I, Gorodin S, Barzilai A, Malik Z, Melamed E: Dopamine-induced programmed cell death in mouse thymocytes. Biochim Biophys Acta 1995;1268:171-177.
52 Roomans GM: Application of X-ray microanalysis to the study of cell physiology in cells attached to biomaterials. Eur Cell Mater 2002;3:1-8.
53 Salido M, Vilches J, Lopez A, Roomans GM: X-ray microanalysis of etoposide-induced apoptosis in the PC-3 prostatic cancer cell line. Cell Biol Int 2001;25:499-508.
54 Skepper JN, Karydis I, Garnett MR, Hegyi L, Hardwick SJ, Warley A, Mitchinson MJ, Cary NR: Changes in elemental concentrations are associated with early stages of apoptosis in human monocyte-macrophages exposed to oxidized low-density lipoprotein: an X-ray microanalytical study. J Pathol 1999;188:100-106.
55 Zabiti S, Arrebola F, Canizares FJ, Cubero MA, Fernández-Segura E, Crespo PV, Campos A: Elemental composition during the apoptotic degradation phase. Int J Dev Biol 2001;45:S163-S164.
56 Hughes FM, Jr., Cidlowski JA: Potassium is a critical regulator of apoptotic enzymes in vitro and in vivo. Adv Enzyme Regul 1999;39:157-171.
57 Segal MS, Beem E: Effect of pH, ionic charge, and osmolality on cytochrome c-mediated caspase-3 activity. Am J Physiol Cell Physiol 2001;281:C1196-C1204.
58 Wenzel U, Daniel H: Early and late apoptosis events in human transformed and non-transformed colonocytes are independent on intracellular acidification. Cell Physiol Biochem 2004;14:65-76.
59 Morán J, Hernández-Pech X, Merchant-Larios H, Pasantes-Morales H: Release of taurine in apoptotic cerebellar granule neurons in culture. Pflugers Arch 2000;439:271-277.
60 Lang PA, Warskulat U, Heller-Stilb B, Huang DY, Grenz A, Myssina S, Duszenko M, Lang F, Haussinger D, Vallon V, Wieder T: Blunted apoptosis of erythrocytes from taurine transporter deficient mice. Cell Physiol Biochem 2003;13:337-346.